# Generating a nonequilibrium stationary state from a ground-state condensate through an almost adiabatic cycle

Atushi Tanaka [1,*] Takaaki Nakamura [2] and Taksu Cheon [2]

[1]*Department of Physics, Tokyo Metropolitan University, Hachioji, Tokyo 192-0397, Japan*
[2]*Laboratory of Physics, Kochi University of Technology, Tosa Yamada, Kochi 782-8502, Japan*

It is shown, through a mean-field description, that the ground state of weakly interacting Bose particles in a quasi-one-dimensional box trap can be converted into an excited stationary state by an almost adiabatic cyclic operation that involves a quench: A sharp impurity potential is applied, and its strength is varied during the cycle, which induces a nonequilibrium stationary state exhibiting the inversion of population. This process is robust in the sense that the resultant stationary state is almost independent of the details of the cycle, such as the position of the impurity, as long as the cycle is far enough from critical regions. The case of the failure of the population inversion due to the strong interparticle interactions is also examined.

## I. INTRODUCTION

According to the principle of the equilibrium thermodynamics, a quasistatic adiabatic cycle is trivial, in the sense that the initial and final states are identical [1]. Once we slightly relieve the quasistatic adiabatic condition or the thermodynamic condition, however, a cyclic operation may transform a stationary state into another one. A promising system to realize such stationary state transformations in a many-body, nearly thermodynamic setting is cold atoms. This is because it is possible to manipulate the system with its quantum coherence intact, as it can be well isolated from environmental degrees of freedom.

An example [2] can be found in the Lieb-Liniger model [3,4], which describes Bose particles confined in a one-dimensional ring. A stationary state of the Lieb-Liniger model is delivered to another stationary state through a cyclic operation where the strength of interparticle interaction is adiabatically increased except at a point: Once the interparticle interaction becomes infinitely repulsive to make the Tonks-Girardeau regime [5], the interparticle interaction strength is flipped to infinitely attractive to form the super-Tonks-Girardeau regime [6,7]. During the cyclic operation, the stationary state is smoothly deformed even at the strength flipping point, where normalizable stationary states are ensured to be kept unchanged.

The state transformations in the Lieb-Liniger model are an example of exotic quantum holonomy in adiabatic cycles of microscopic, nonthermal systems: Although one may expect that an adiabatic cycle brings no change in stationary states up to a phase factor, it may transform a stationary state into another, for example, in Floquet systems through the winding of quasienergy [8–10] and Hamiltonian systems with level crossings [11,12]. A concept similar to, but distinct from, the exotic quantum holonomy, Wilczek-Zee holonomy, where an adiabatic cycle offers a transformation of degenerated stationary states [13–15], is also utilized to control quantum states [16–18].

We note that the adiabatic state transformation in the Lieb-Liniger model [2] heavily depends on the particularity of the model. The number of particles is required to be specified precisely. Also, the theoretical argument in Ref. [2] depends essentially on the solvability of the system. Hence it seems difficult to extend this result to other quantum many-body systems.

In this paper, we examine an adiabatic state transformation in a quantum many-body system through a mean-field description to mitigate this difficulty. Applying an almost adiabatic cycle that involves a quench of the strength of a sharp impurity potential to the bosons in the ground state, we obtain an excited stationary state, which is called a population-inverted state. Namely, the bosons, under the mean-field description, occupy a single-particle excited state. The population inversion has been utilized to achieve negative temperature [19]. In studies of the collective excitation of Bose-Einstein condensates, it has been recognized that such excited stationary states present dark solitons, and thus they have been extensively examined. An adiabatic method that involves internal atomic states was proposed to produce the dark solutions in Ref. [20]. Later, another adiabatic method that involves a sweep of an additional potential well was studied [21,22]. The latter method was extended to Fermi gases [23] and two-dimensional rotating condensates to produce vortices [24].

In this work, our starting point is the analysis of cyclic operations for noninteracting Bose particles [25,26]. Apart from the point where the adiabatic path is closed or open, a notable difference of the present approach from the previous proposals mentioned above is that it is free from narrow

───────
*http://researchmap.jp/tanaka-atushi/

avoided crossings without referring to the multiple internal atomic states [20–22]. The Bose particles are confined in a quasi-one-dimensional box trap [27–30]. We define a cycle using a sharp impurity potential, which can be realized by a laser beam [21,31]. Sharp potentials have been utilized to manipulate superfluids [31–33] and dark solitons [34,35]. In order to incorporate the interparticle interaction, we suppose that the system is described by the time-dependent Gross-Pitaevskii equation. We show that the interparticle interaction can significantly modify the almost adiabatic processes due to the appearance of bifurcations in the solution of time-independent Gross-Pitaevskii equation such as the swallowtail structure [22,36–40].

The plan of this paper is the following. In Sec. II, we introduce a cyclic operation that involves a flip of the potential strength which is analogous to the cyclic operation introduced in Ref. [25] for noninteracting systems. In Sec. III, we numerically examine the cyclic operation in the repulsively interacting Bose particles using the Gross-Pitaevskii equation, where it is shown that the strong nonlinearity disturbs the population inversion. In Sec. IV, a theoretical interpretation for the numerical result is shown. Section V concludes this paper with a summary and outlook. The Appendix offers details of the linear stability analysis (the Bogoliubov analysis) at the quench point.

## II. CYCLE FOR NONINTERACTING PARTICLES

We look at a cyclic operation for particles confined in a quasi-one-dimensional boxed trap with an impurity potential. We illustrate how this cycle works for noninteracting particles [25], which offers a basis for examining the case of interacting bosons.

We assume that a particle is described by the one-dimensional time-dependent Schrödinger equation

$$i\hbar \frac{\partial}{\partial t} \Psi(x,t) = -\frac{\hbar^2}{2M} \frac{\partial^2}{\partial x^2} \Psi(x,t) \qquad (1)$$

under the boundary condition $\Psi(0,t) = \Psi(L,t) = 0$, where $M$ is the mass of the particle and $L$ is the size of the box trap. In the following, we assume $\hbar = 1$, $M = 1/2$, and $L = 2\pi$.

After the system is prepared to be in a stationary state, i.e., an eigenstate of the Hamiltonian, a sharp impurity potential is placed at $x = X$ to realize cyclic operations, where the strength $v$ is varied. We assume that the impurity potential $V_i(x; v)$ is described by the Dirac delta function:

$$V_i(x; v) = v\delta(x - X). \qquad (2)$$

During the cycle, the system is described by the time-dependent Schrödinger equation

$$i\hbar \frac{\partial}{\partial t} \Psi(x,t) = \left\{ -\frac{\hbar^2}{2M} \frac{\partial^2}{\partial x^2} + V_i(x; v(t)) \right\} \Psi(x,t), \quad (3)$$

where the time-dependent parameter $v(t)$ is specified in the following.

There are two building blocks of the cyclic operation: One is the smooth and monotonic variations of parameter $C_s(v', v'')$, which denotes the variation of $v$ from $v'$ to $v''$ while keeping the value of $X$ constant. To realize the adiabatic time evolution $C_s(v', v'')$, the time dependence of the parameter
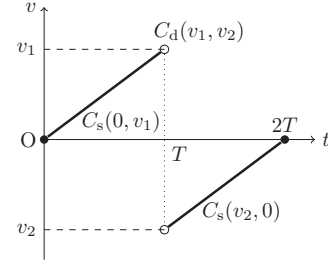


FIG. 1. An example, shown in Eq. (6), of the time dependence of $v(t)$, the strength of the impurity potential [Eq. (2)], along the closed path $C(X)$, which consists of $C_s(0, v_1)$, $C_d(v_1, v_2)$, and $C_s(v_2, 0)$. Throughout the cycle, the position $X$ of the impurity potential is fixed. The cycle is supposed to be adiabatic (i.e., $T$ is large enough), except at $t = T$, where $v(t)$ is quenched from $v_1$ to $v_2$. In the limit $v_1 \to \infty$ and $v_2 \to -\infty$, the quench operation smoothly connects the eigenstates. In numerical experiments, we assume that the absolute values of $v_1$ and $v_2$ are large, but finite.

$v(t)$ is, for example,

$$v(t) = \frac{t'' - t}{t'' - t'} v' + \frac{t - t'}{t'' - t'} v', \qquad (4)$$

where $t'$ and $t''$ are the initial and final times, respectively, and $t'' - t'$ needs to be large enough. The other is the discontinuous operation $C_d(v', v'')$ in which the value of $v$ is changed from $v'$ to $v''$, which resembles the process that is utilized to create the super-Tonks-Girardeau gas from the Tonks-Girardeau gas [7]. The time dependence of the parameter $v(t)$ for the operation $C_d(v', v'')$ is, for example,

$$v(t) = \begin{cases} v' & \text{for} \quad t \leqslant t_d, \\ v'' & \text{for} \quad t > t_d, \end{cases} \qquad (5)$$

where the operation $C_d(v', v'')$ is carried out at $t = t_d$. The details of these operations, e.g., the parameters $t'$, $t''$, and $t = t_d$, need to be chosen appropriately to compose a cycle from the building blocks, as shown below.

We define the almost adiabatic cyclic operation $C(X)$ (see Fig. 1), which involves a quench of the impurity potential placed at $X$. This cycle is a succession of three operations, $C_s(0, \infty)$, $C_d(\infty, -\infty)$, and $C_s(-\infty, 0)$. This can be approximately realized by a succession of three operations, $C_s(0, v_1)$, $C_d(v_1, v_2)$, and $C_s(v_2, 0)$, where the absolute values of $v_1 > 0$ and $v_2 < 0$ are supposed to be large enough. To realize the almost adiabatic evolution, the time dependence of $v(t)$ is, for example,

$$v(t) = \begin{cases} \frac{t}{T} v_1 & \text{for} \quad 0 \leqslant t \leqslant T, \\ \frac{2T - t}{T} v_2 & \text{for} \quad T < t \leqslant 2T, \end{cases} \qquad (6)$$

where $T$ needs to be large enough to ensure nonadiabatic transitions are small enough.

We show that an initial eigenstate $\Psi_n(x)$ can be transformed to another eigenstate after the completion of a cycle. Here we assume that the parameters are varied adiabatically during the smooth operations. Hence the system is governed by the adiabatic theorem [41]. Since the relevant eigenenergy and eigenfunction are continuous during the quench, the parametric dependence of eigenenergies tells us the final
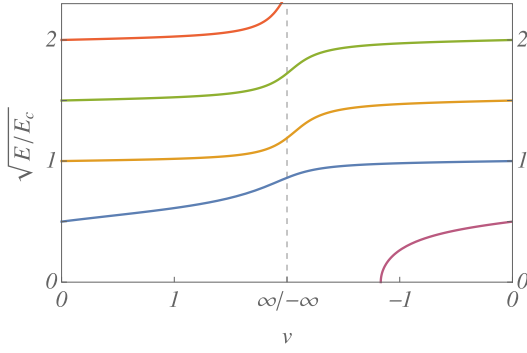
FIG. 2. Parametric evolution of eigenenergies along $C(X = 0.42L)$, which connects the $n$th and $(n+1)$th eigenenergies. The horizontal axis is linear in $\tan^{-1} v$. We define $E_c \equiv (2\pi\hbar/L)^2/(2M)$ to depict the eigenenergies.

eigenstate for the almost adiabatic cycle $C(X)$. We depict an example of the parametric evolution of eigenenergies in Fig. 2.

After the completion of the almost adiabatic cycle $C(X)$, the final state is $\Psi_{n+1}(x)$, as long as $X$ does not coincide with the node of the initial wave function $\Psi_n(x)$. This is because the eigenenergies are increased monotonically during $C_s(0, \infty)$ and $C_s(-\infty, 0)$ as $v$ is increased monotonically [25,42] and are continuous at the quench process $C_d(\infty, -\infty)$ [25].

Let us extend the above argument to the noninteracting Bose particles. Suppose that all particles occupy the single-particle ground state $\Psi_1(x)$. After the completion of the almost adiabatic operation $C(X)$, all particles occupy the first excited state $\Psi_2(x)$. Namely, a population-inverted state can be created from the ground state through the almost adiabatic operation $C(X)$.

Although the almost adiabatic cycle $C(X)$ induces exotic changes as shown above, the cycle involves several idealizations. In particular, we need to take into account the effect of interparticle interaction. In the following sections, we scrutinize the almost adiabatic cyclic operation $C(X)$ for interacting Bose particles.

## III. CYCLE FOR AN INTERACTING BOSE SYSTEM

We here examine the almost adiabatic cycle $C(X)$ in a many-body setting. We assume that Bose particles are confined in the quasi-one-dimensional box and the interparticle interaction is repulsive. First, we examine the parametric evolution of stationary states along the cycle, which suggests that the population inversion is, indeed, possible if the interparticle interaction is weak. Also, it is shown that the population inversion breaks down when the interparticle interaction is strong enough. Second, we numerically integrate the time-evolution equation to confirm the picture obtained through the parametric evolution of the stationary states. We provide a theoretical explanation based on a perturbation theory to these observations in the next section.

We assume that the Bose particles are described by the time-dependent one-dimensional Gross-Pitaevskii equation

$$i\frac{\partial}{\partial t}\Psi(x,t) = -\frac{\partial^2}{\partial x^2}\Psi(x,t) + g|\Psi(x,t)|^2\Psi(x,t), \quad (7)$$
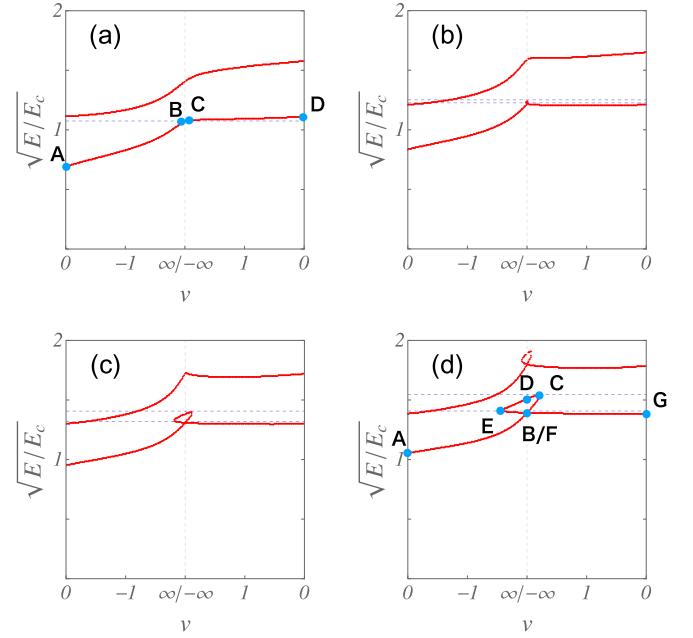


FIG. 3. Parametric evolution of the ground and first excited eigenenergies (chemical potentials) along $C(X = 0.42L)$. The horizontal axis is linear in $\tan^{-1} v$. (a) The eigenenergies form smooth and monotonic curves at $g = 1$, which are similar to the case $g = 0$. (b) A tiny loop around $|v| = \infty$ appears in the ground energy curve at $g = 2$. (c) The loop of the ground energy grows at $g = 3$, while the derivative of the first excited energy seems to be discontinuous at $|v| = \infty$. (d) There are two noticeable loops at $g = 4$. Blue dotted lines are the eigenenergies estimated by the two-mode approximation (see Sec. IV) of the ground branch at $|v| = \infty$. $E_c$ is defined in the caption of Fig. 2.

where $\hbar = 1$, $M = 1/2$, and $L = 2\pi$ are assumed and $g \geqslant 0$ represents the strength of the effective interparticle interaction. We impose the boundary condition $\Psi(0, t) = \Psi(L, t) = 0$ and the normalization condition $\int_0^L |\Psi(x, t)|^2 dx = 1$. Let $E_n(g)$ and $\Psi_n(x; g)$ $(n = 1, 2, \ldots)$ denote the $n$th eigenenergy (chemical potential) and the corresponding stationary state for Eq. (7). We suppose that the system is initially in the $n$th stationary state $\Psi_n(x; g)$. During the cycle, we impose the sharp impurity potential [Eq. (2)] to Eq. (7) and vary its strength $v$ slowly except at the quench point.

To find the stationary states of the system where the position $X$ and strength $v$ of the impurity potential [Eq. (2)] are "frozen," we examine the time-independent Gross-Pitaevskii equation with the impurity potential

$$\left(-\frac{\partial^2}{\partial x^2} + g|\Psi(x)|^2 + V_i(x; v)\right)\Psi(x) = E\Psi(x). \quad (8)$$

Examples of parametric evolution of the $n$th eigenenergy along the cycle $C(X)$ are shown in Fig. 3. Corresponding parametric evolution of stationary states is shown in Figs. 4 and 5.

When the interparticle interaction $g$ is small enough, the almost adiabatic cyclic operation induces the population inversion. The parametric evolution of eigenenergy along the cycle connects the initial eigenenergy $E_1(g)$ with $E_2(g)$ [see Fig. 3(a)]. The connection is equivalent to the case of
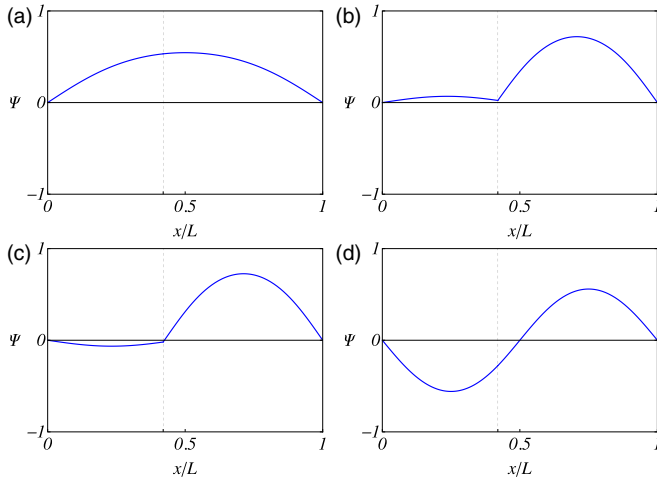
FIG. 4. Parametric evolution of stationary state $\Psi(x)$ of weakly interacting Bose particles along the cycle $C(X = 0.42L)$ and $g = 1$. The corresponding points in $(g, E)$ plane is shown in Fig. 3(a) (points A–D). (a) $\Psi(x)$ is the ground state initially (i.e., $v = 0$, point A); (b) and (c) correspond to the cases immediately before (point B) and after (point C) the quench. (d) The final state is the first excited state (point D). The phase of $\Psi(x)$ is chosen so that $\Psi(x)$ is positive on the right-hand side of the sharp impurity. The dashed vertical lines indicate the position $X$ of the impurity potential [Eq. (2)].

noninteracting particles (see Fig. 2). This allows us to infer the parametric evolution of the eigenfunction whose initial condition is the ground state $\Psi_1(x; g)$ of Eq. (7), i.e., at $g = 0$ [see Fig. 4(a)]. While the stationary state is nodeless when the strength of the sharp impurity potential $v$ is positive and finite, the state becomes localized on a side of the impurity as $v$ become larger [Fig. 4(b)]. Immediately before the quench, i.e., $v = \infty$, the localization is completed [43]. The state is unchanged during the flip of the potential strength from $v = \infty$ to $v = -\infty$ [25]. As $v$ is slightly increased from $-\infty$, the stationary state extends to the other side of the impurity to produce a node [Fig. 4(c)]. The resultant stationary state has a single node while $v$ is finite [Fig. 4(d)]. This is the reason why the destination of the stationary state at the end of the cycle is the first excited state $\Psi_2(x; g)$.

On the other hand, when the interparticle interaction is large, discrepancies from the linear case become significant. In particular, as is seen in Figs. 3(c) and 3(d), the parametric evolution of a stationary energy involves a loop structure that emanates from the quench point $|v| = \infty$ in $C(X)$. We note that loop structures are often observed in studies of time-independent Gross-Pitaevskii equation [22,36–39].

The corresponding parametric evolution of the stationary state along the loop is explained in the following. The stationary states shown in Fig. 5 correspond to the points A–G in Fig. 3(d). In the vicinity of the quench, the wave function extends to both sides of the sharp impurity potential, which is a distinctive feature of the case with stronger interparticle interaction (point $B_+$). Across the quench point the wave function smoothly connects to the lower branch of the loop to acquire two nodes (point $B_-$). As $v$ increases, the lower branch arrives at the extremum point (point C) to connect the uppermost branch, where the wave function localizes on a side
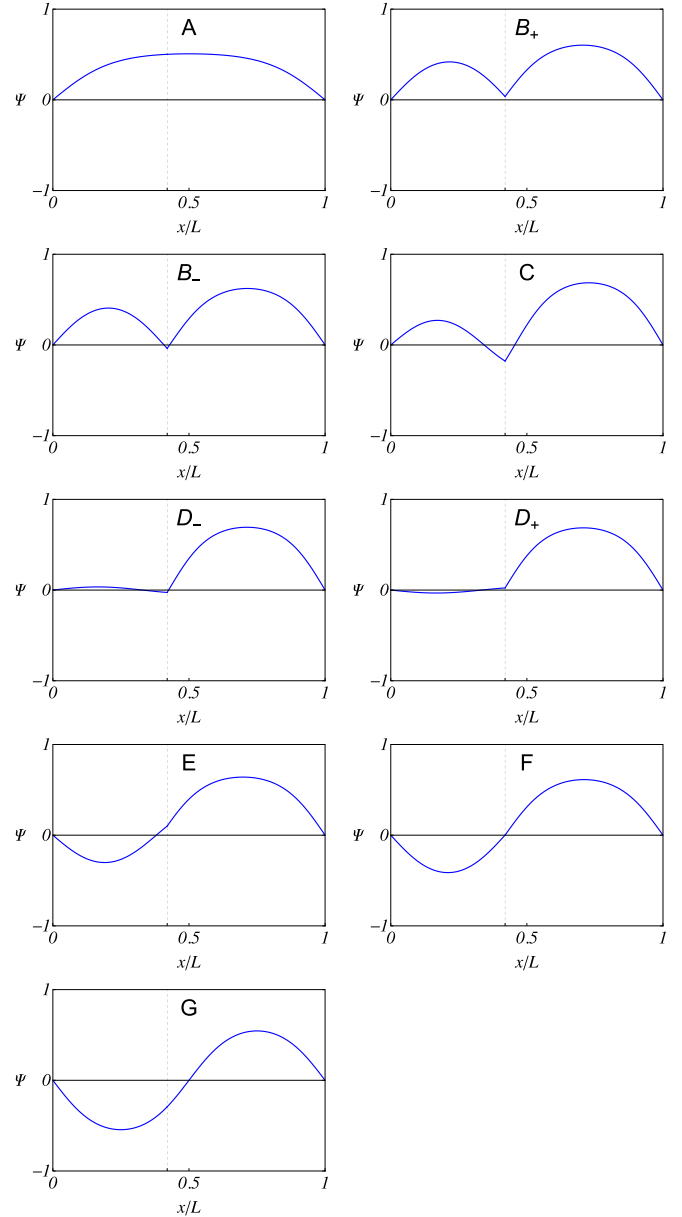


FIG. 5. Parametric evolution of stationary state $\Psi(x)$ along an eigenenergy loop associated with the cycle $C(X = 0.42L)$ at $g = 4$, which corresponds to the case shown in Fig. 3(d). The loop connects the initial point A and the final point G of the cycle $C(X)$. Around the quench points B and D, the sign of $v$ is indicated by the subscript $\pm$. The dashed vertical lines indicate the position $X$ of the impurity potential [Eq. (2)].

of the impurity potential, where the stationary state mimics the one in the linear system. As $v$ decreases to follow the uppermost branch, the stationary state becomes localized on a side of the impurity (point $D_-$). At the quench point in the uppermost branch, the localization is completed. Across the quench, the number of nodes of the stationary state decreases from 2 ($D_-$) to 1 ($D_+$). Then the uppermost branch arrives at another extremum point (point E), where the stationary state delocalizes again to connect the final branch at point F, which smoothly connects the first excited state $\Psi_2(x; g)$ (see point G).

We expect that the loop structure disturbs the adiabatic evolution, as reported in Refs. [36,37], and thus hinders the population inversion. This is because the stationary state is transformed into a nonstationary state when the adiabatic time evolution has to depart from the parametric evolution by having a loop.

To clarify whether the adiabatic time evolution along $C(X)$ really occurs, we numerically examine the linear stability of the stationary states in $C(X)$ by diagonalizing the Bogoliubov equation [44,45] corresponding to the stationary solutions. Also, an analytical study of the linear stability for the quench point is shown in the Appendix.

When the interparticle interaction is small [see Figs. 3(a) and 4], we find that the stationary states are linearly stable along $C(X)$. Hence we may expect the adiabatic time evolution to remain intact for the weakly interacting case.

Meanwhile, when the interparticle interaction is large enough to form the loop structure shown in Figs. 3(d) and 5, we find that the stationary state is linearly stable within the intervals from $v = 0$ through $v = \pm\infty$, i.e., from A to B and from G to F in Fig. 3(d), and the uppermost branch of the loop (from C to E). On the other hand, the stationary state is linearly unstable in the lower part of the loop (i.e., from B to C and E to F).

The result of the linear stability analysis for stronger interparticle interaction suggests that the adiabatic time evolution whose initial condition is the ground state $\Psi_1$ remains intact until the quench point, i.e., within the interval A to B. After the system passes the quench point, the adiabatic time evolution breaks down during the interval B to C due to the linear instability. We note that the emergence of the unstable stationary state in the lower branch of the loop structure in the Brillouin zone is reported in Refs. [46,47]. We also note that this is a distinctive point from the instabilities in the conventional studies [36,37] of adiabatic time evolution along the loop structure, where the linearly unstable region appears only in the uppermost part of the loop structure. After point C, the adiabatic time evolution is impossible since the stationary solution cannot be adiabatically extended anymore [36,37].

We test the scenario above through numerical integration of the time-dependent Gross-Pitaevskii equation along the almost adiabatic cycle $C(X)$. We show our numerical result for various values of $X$ in Fig. 6, where the initial condition is prepared to be in the ground state $\Psi_1(x; g)$ of Eq. (7). We numerically evaluate the fidelity of the population inversion $|\langle \Psi_2(g)|\Psi\rangle|^2$, where $\Psi$ is a state after the completion of the cycle. Since the final states may not be stationary, we depict the time average of the fidelity probability after the completion of the cycles.

From Fig. 6, we conclude that the population inversion fails if the value of $g$ exceeds a critical value $g_c$, which depends on the position of the impurity potential $X$. Moreover, when we restrict ourselves to the case $0 < X < L/2$, $g_c$ becomes larger as $X$ become smaller.

We make a remark on the integration of the time-dependent Gross-Pitaevskii equation along $C(X)$, where we introduce an approximation for the quench of the impurity potential. We keep $v$, the strength of the impurity potential, finite. Namely, $v$ is increased from zero to $v_{\max}$ with a finite velocity $dv/dt$ during the first process $C_s(0, v_{\max})$. At the quench,
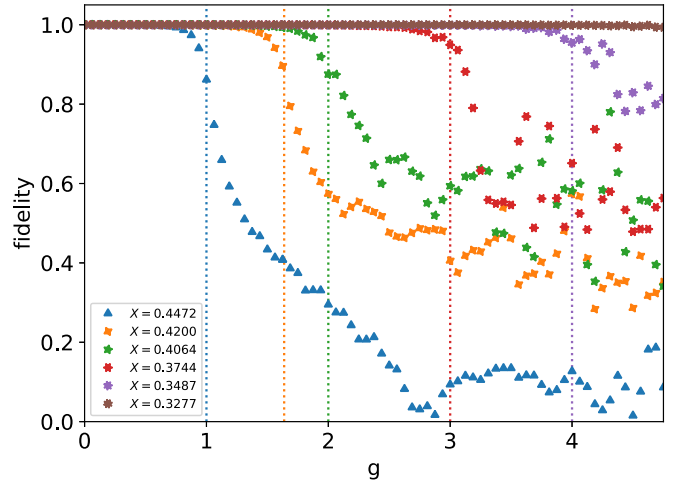


FIG. 6. Population inversion probability from the ground state through $C(X)$. Vertical dashed lines indicate the critical point predicted by the two-mode approximation (see Sec. IV).

$v$ is suddenly changed from $v_{\max}$ to $-v_{\max}$. Then, during $C_s(-v_{\max}, 0)$, the value of $v$ is increased from $-v_{\max}$ to zero with nonzero velocity $dv/dt$. Although this induces a tiny nonadiabatic error during the quench, as seen in Fig. 6, the error is far less important than the nonlinear effect.

## IV. TWO-MODE APPROXIMATION AT THE QUENCH POINT

We discuss our numerical results in the previous section with an approximate theory. In particular, we would like to clarify the reason why the population inversion breaks down as the strength of the interparticle interaction becomes stronger (Fig. 6). A key ingredient must be the emergence of the loop in the $(g, E)$ plane (Fig. 3). To identify the loop structure, we examine the quench point $|v| = \infty$ because a loop emanates from a point at $|v| = \infty$ in the $(g, E)$ plane. This analysis allows us to infer the loop structure, as long as the loop is small enough.

In the following, we utilize a two-mode approximation. Namely, we assume that the stationary wave function $\Psi(x)$ is a superposition of two eigenfunctions $\psi_j(x)$ ($j = 0, 1$) of the noninteracting system. Since the infinitely strong impurity divides the box completely [43], as suggested in Fig. 3, we utilize the unperturbed eigenfunction $\psi_j(x)$ that is localized on the left or right side of the impurity.

For example, to examine the stationary states that are associated with the ground state at the initial point of the cycle, we assume that $\psi_0(x)$ and $\psi_1(x)$ describe the ground state of a single particle confined within the right and left boxes, respectively, i.e.,

$$\psi_0(x) = \begin{cases} 0 & \text{for } 0 \leqslant x \leqslant X, \\ \sqrt{\frac{2}{L-X}} \sin \frac{\pi(x-X)}{L-X} & \text{for } X \leqslant x \leqslant L, \end{cases} \quad (9)$$

$$\psi_1(x) = \begin{cases} \sqrt{\frac{2}{X}} \sin \frac{\pi x}{X} & \text{for } 0 \leqslant x \leqslant X, \\ 0 & \text{for } X \leqslant x \leqslant L, \end{cases} \quad (10)$$

whose eigenenergies are $E_0 = E_{\mathrm{g}}/r'^2$ and $E_1 = E_{\mathrm{g}}/r^2$, respectively, where $r = X/L$, $r' = (L - X)/L$, and $E_{\mathrm{g}} = \hbar^2\pi^2/(2ML^2)$.

In the following, we assume $0 < X < L/2$, which implies $E_0 < E_1$; that is, the ground state $\psi_0(x)$ in the presence of the infinitely strong impurity localizes on the right side of the impurity.

From the two-mode assumption that $\Psi(x, t) = \Psi_0(t)\psi_0(x) + \Psi_1(t)\psi_1(x)$ satisfies the time-dependent Gross-Pitaevskii equation, we obtain the time-evolution equation for the amplitudes $\Psi_j(t)$ $(j = 0, 1)$:

$$i\frac{d}{dt}\Psi_j(t) = E_j\Psi_j(t) + g\int_0^L \psi_j^*(x)|\Psi(x, t)|^2\Psi(x, t)dx. \tag{11}$$

Because $\psi_0(x)$ and $\psi_1(x)$ have no overlap in position space, i.e., $\psi_0(x)\psi_1(x) = 0$ holds, and are real, we obtain

$$i\frac{d}{dt}\Psi_j = E_j\Psi_j + g\int_0^L dx\{\psi_j(x)\}^4|\Psi_j|^2\Psi_j. \tag{12}$$

Hence the nonlinear Schrödinger equation for $\Psi_j$ is

$$i\frac{d}{dt}\Psi_j = (E_j + gc_j|\Psi_j|^2)\Psi_j, \tag{13}$$

where $c_0 \equiv 3g/\{2(L - X)\}$ and $c_1 \equiv 3g/(2X)$. We also impose the normalization condition $|\Psi_0|^2 + |\Psi_1|^2 = 1$.

The stationary solutions of Eq. (13) are classified into two groups. First, there are two localized solutions $(\Psi_0, \Psi_1) = (1, 0)$ and $(0,1)$, whose eigenenergies are

$$E_0(g) = E_0 + gc_0, \quad E_1(g) = E_1 + gc_1, \tag{14}$$

respectively.

Second, the other two solutions $\Psi_\pm$ are

$$\begin{bmatrix} \Psi_{\pm,0} \\ \Psi_{\pm,1} \end{bmatrix} = \begin{bmatrix} \sqrt{r' - (E_0 - E_1)(2Lrr')/(3g)} \\ \pm\sqrt{r + (E_0 - E_1)(2Lrr')/(3g)} \end{bmatrix}, \tag{15}$$

which are delocalized on both sides of the impurity. The corresponding eigenenergies are doubly degenerate,

$$E_\pm(g) = r'E_0 + rE_1 + \frac{3g}{2L}. \tag{16}$$

We explain the condition that the stationary states (15) are physical, i.e., $0 \leqslant |\Psi_0|^2, |\Psi_1|^2 \leqslant 1$ hold. First, we introduce the critical points

$$g_0 = \frac{2(L - X)}{3}(E_1 - E_0), \tag{17}$$

$$g_1 = -\frac{2X}{3}(E_1 - E_0), \tag{18}$$

where $|\Psi_j|^2 = 1$ holds if $g = g_j$ $(j = 0, 1)$. Since we assume $X < L/2$, the physical condition for the stationary solution (15) is summarized as $g \geqslant g_0$ or $g \leqslant g_1$. Also, as we restrict ourselves to the case in which the interparticle interaction is repulsive, i.e., $g \geqslant 0$, the delocalized solutions (15) exist only when $g \geqslant g_0$.

From the linear stability analysis (Bogoliubov analysis) of Eq. (13), whose details are shown in the Appendix, we find that the localized solutions $(\Psi_0, \Psi_1) = (1, 0)$ and $(0,1)$ are stable. On the other hand, the delocalized solutions (15) are marginally stable.

With the two-mode approximation at $|v| = \infty$, we recapitulate the parametric evolution of stationary states and eigenenergies along $C(X)$. We assume that the system is initially in the ground state $\Psi_1(x; g)$.

First, we revisit the case in which the interparticle interaction is weak enough, i.e., $g$ is smaller than the critical value $g_0$. The stationary state is localized at $|v| = \infty$, which is consistent with Fig. 4. The corresponding estimation of eigenenergy at $|v| = \infty$ is given by Eq. (14), which is indicated in Fig. 3. Also, the stationary state at $|v| = \infty$ is stable, according to the linear stability analysis. Hence the stationary state must be stable during $C(X)$, which is also consistent with the numerical result that $C(X)$ induces the population inversion for smaller $g$ (Fig. 6).

Second, when the strength of the interparticle interaction $g$ exceeds the critical value $g_0$, the localized and delocalized stationary solutions coexist at the quench point: the degenerate eigenenergies of the delocalized solutions $E_\pm(g)$ [Eq. (16)] are lower than that of the localized solution [Eq. (14)], as shown in Fig. 3. The delocalized nodeless solution $\Psi_+$ (Fig. 5, points $B_\pm$) is connected to the initial ground state $\Psi_1$ through $C_s(0, \infty)$, the former half of the whole cycle. After $\Psi_+$ evolves along the loop, the stationary solution arrives at the localized solution $(\Psi_0, \Psi_1) = (1, 0)$ at $|v| = \infty$ (see Fig. 5, points $D_\pm$). After the completion of the loop, the stationary solution becomes another delocalized solution $\Psi_-$ with a node (Fig. 5, point F). The latter half of the cycle $C_s(-\infty, 0)$ smoothly connects $\Psi_-$ to the first excited state $\Psi_2$. In this sense, the parametric evolution of the stationary solution smoothly deforms the ground state into the first excited state. Meanwhile, the adiabatic population inversion is hindered by the presence of the loop structure due to the instability of the stationary state at the lower branch of the loop, as explained in the previous section.

In Fig. 6, we indicate the critical interparticle interaction strength $g_0$, which is estimated by the two-mode approximation for each value of $X$ by vertical lines. Hence we conclude that the two-mode approximation qualitatively describes the breakdown of the population inversion.

We depict how the eigenenergies at the quench point depend on the position $X$ of the sharp impurity in Fig. 7 using the two-mode approximation. This helps us to understand the cycle $C(X)$ for a given value of $g$. For example, at $X = 0.42L$, the ground branch connected to a loop whose section at $v = |\infty|$ has two delocalized and one localized stationary states, which predicts the breakdown of the population inversion to the first excited state. Also, the first (second) excited state at the initial point of the cycle is connected to a localized stationary state, which suggests that the population inversion to the second (third) excited state may be possible.

## V. SUMMARY AND OUTLOOK

We have shown that the adiabatic cyclic operation with a quench $C(X)$ induces the population inversion of Bose particles described by the Gross-Pitaevskii equation confined in a quasi-one-dimensional box if the Bose particles are initially prepared to be in the ground state and the strength $g$ of the interparticle interaction is weak enough. An estimation of the critical value of $g$ where the population inversion is
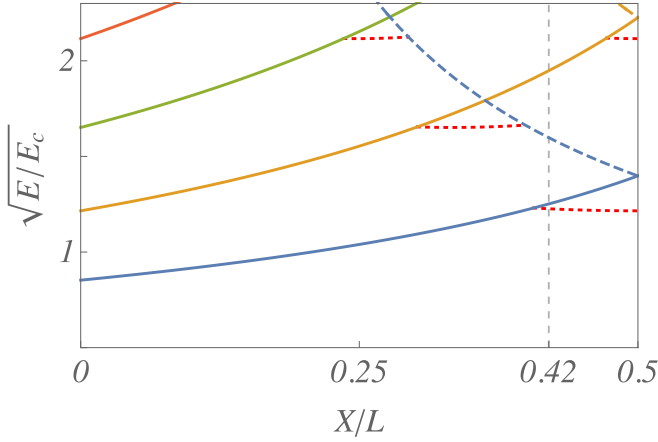
FIG. 7. $X$ dependence of stationary energies at the quench $|v| = \infty$ and $g = 2$ under the two-mode approximation. The solid (dashed) lines correspond to the stable stationary states localized on the right (left) side of the infinitely strong impurity. The dotted lines correspond to the delocalized stationary states that are marginally stable. $E_c$ is defined in the caption of Fig. 2.

broken is also shown. We find that these results are consistent with our numerical investigation through the time-dependent Gross-Pitaevskii equation.

We note that the time evolution generated by the almost adiabatic operation $C(X)$ can confine the system within a family of stationary states in the weak-interaction regime. Namely, the adiabatic time evolution can be realized in spite of the presence of the flip of the potential strength at the quench point. This "adiabatic" cycle converts the ground state of Bose particles into a nonequilibrium stationary state. The present study offers an example of the subtle difference between the adiabatic processes in thermodynamic systems and nonthermal, mechanical systems.

We believe that the present result offers an experimentally feasible method to produce a nonequilibrium stationary state. Application of the acceleration of the adiabatic scheme to the present procedure (e.g., Refs. [48,49]) should also be interesting. We note that the preparation of condensates in a quasi-one-dimensional box trap was experimentally achieved in Ref. [27], which motives theoretical studies, e.g., on solitonic excitations [30]. We also remark that the box trap may be useful to investigate quantum information processing through, e.g., the Szilard engine in the quantum regime [50,51]. To extend these works to many-body settings, our analysis of the infinitely strong impurity should be applicable.

*Note added.* Recently, the state transformation due to an almost adiabatic cycle for the Lieb-Liniger system [2] was extended to the one-dimensional dipolar Bose gas to create its long-lived excited states [52].

## APPENDIX: LINEAR STABILITY ANALYSIS FOR THE TWO-MODE SYSTEM (13) AT THE QUENCH POINT

We explain the linear stability analysis (Bogoliubov analysis) of the stationary states at the quench point in $C(X)$. To carry this out, the nonlinear Schrödinger equation (13) under the two-mode approximation is cast into a nonlinear Bloch equation [Eq. (A3) below]. The components of the Bloch vector $\boldsymbol{S} = (S_x, S_y, S_z)$ are the expectation values of Pauli matrices $\sigma_j$ for a normalized state $(\Psi_0, \Psi_1)$, e.g., $S_z = |\Psi_0|^2 - |\Psi_1|^2$.

To find the time-evolution equation of $\boldsymbol{S}$, we first obtain a matrix form of Eq. (13). The system is described by an effective nonlinear Hamiltonian $H_2 = \Delta_+ I + \Delta_- \sigma_z$, where $I$ is the identity matrix and

$$\Delta_\pm(\boldsymbol{S}) \equiv \frac{1}{2}\left\{\left(E_0 + gc_0\frac{1+S_z}{2}\right) \pm \left(E_1 + gc_1\frac{1-S_z}{2}\right)\right\}. \tag{A1}$$

Hence $\boldsymbol{S}$ experiences the effective magnetic field

$$\boldsymbol{B}(\boldsymbol{S}) \equiv \Delta_-(\boldsymbol{S})\boldsymbol{e}_z, \tag{A2}$$

where $\boldsymbol{e}_z \equiv (0, 0, 1)$. Namely, $\boldsymbol{S}$ obeys the nonlinear Bloch equation

$$\frac{d}{dt}\boldsymbol{S} = \boldsymbol{S} \times \boldsymbol{B}(\boldsymbol{S}). \tag{A3}$$

A stationary state of Eq. (13) corresponds to a stationary solution $\boldsymbol{S}_*$ of Eq. (A3), where $\boldsymbol{S}_* \times \boldsymbol{B}(\boldsymbol{S}_*) = 0$ holds.

We proceed to the linear stability analysis for a stationary solution $\boldsymbol{S}_*$ to examine a slightly perturbed Bloch vector $\boldsymbol{S} = \boldsymbol{S}_* + \delta\boldsymbol{S}$. We expand $\delta\boldsymbol{S}$, using an orthogonal system $\boldsymbol{e}_0 \equiv \boldsymbol{S}_*$, $\boldsymbol{e}_1 \equiv \boldsymbol{e}_y$ [$= (0, 1, 0)$], and $\boldsymbol{e}_2 \equiv \boldsymbol{e}_0 \times \boldsymbol{e}_1$, as

$$\delta\boldsymbol{S} = \alpha_1\boldsymbol{e}_1 + \alpha_2\boldsymbol{e}_2, \tag{A4}$$

where small coefficients $\alpha_j$ are taken up to first order ($j = 1, 2$). The absence of the $\boldsymbol{e}_0$ component in Eq. (A4) is consistent with the normalization condition up to first order. The linearized equation for $\alpha_j$ is

$$\frac{d}{dt}\alpha_j = \boldsymbol{e}_j \cdot \{[\delta B]\boldsymbol{e}_z \times \boldsymbol{S}_* + B_*\boldsymbol{e}_z \times \delta\boldsymbol{S}\}, \tag{A5}$$

where $B_* \equiv \Delta_-(\boldsymbol{S}_*)$, $\delta B = g(c_0 + c_1)S_{*z}\alpha_2/4$, and $S_{*j} = \boldsymbol{S}_* \cdot \boldsymbol{e}_j$ ($j = x, y, z$), from Eqs. (A2) and (A1). Hence we obtain

$$\frac{d}{dt}\begin{bmatrix}\alpha_1 \\ \alpha_2\end{bmatrix} = M\begin{bmatrix}\alpha_1 \\ \alpha_2\end{bmatrix}, \tag{A6}$$

where

$$M \equiv \begin{bmatrix} 0 & -B_* S_{*z} + g\frac{c_0+c_1}{4}S_{*x}^2 \\ B_* S_{*z} & 0 \end{bmatrix}. \tag{A7}$$

We examine $M$ for each stationary solution $\boldsymbol{S}_*$. First, we examine the localized solutions $\boldsymbol{S}_* = \pm\boldsymbol{e}_z$, where

$$M = \pm B_*\begin{bmatrix} 0 & -1 \\ 1 & 0 \end{bmatrix} \tag{A8}$$

and $B_*$ is nonzero, except at the bifurcation point. Since the eigenvalues of $M$ are purely imaginary, the perturbation $\delta S$ evolves oscillatorily and does not grow exponentially in time. Hence we conclude that the stationary solutions $\boldsymbol{S}_* = \pm\boldsymbol{e}_z$ are linearly stable.

Second, we examine the delocalized solution (15), which implies $B_* = 0$. We find

$$M = g\frac{c_0 + c_1}{4}S_{*x}^2\begin{bmatrix} 0 & 1 \\ 0 & 0 \end{bmatrix}, \tag{A9}$$

which is nonzero, except at the bifurcation point. Namely, $M$ has a nontrivial Jordan block and cannot be diagonalized. In terms of dynamical systems, the stability of the delocalized solutions (15) is marginal. Although the perturbation $\delta S$ does not grow exponentially fast, it grows linearly in $t$.

[1] H. B. Callen, *Thermodynamics and an Introduction to Thermostatics*, 2nd ed. (Wiley, New York, 1985).

[2] N. Yonezawa, A. Tanaka, and T. Cheon, Phys. Rev. A **87**, 062113 (2013).

[3] E. H. Lieb and W. Liniger, Phys. Rev. **130**, 1605 (1963).

[4] X. Guan, Int. J. Mod. Phys. B **28**, 1430015 (2014).

[5] M. Girardeau, J. Math. Phys. **1**, 516 (1960).

[6] G. E. Astrakharchik, J. Boronat, J. Casulleras, and S. Giorgini, Phys. Rev. Lett. **95**, 190407 (2005).

[7] E. Haller, M. Gustavsson, M. J. Mark, J. G. Danzl, R. Hart, G. Pupillo, and H.-C. Nägerl, Science **325**, 1224 (2009).

[8] A. Tanaka and M. Miyamoto, Phys. Rev. Lett. **98**, 160407 (2007).

[9] T. Kitagawa, E. Berg, M. Rudner, and E. Demler, Phys. Rev. B **82**, 235114 (2010).

[10] L. Zhou, C. Chen, and J. Gong, Phys. Rev. B **94**, 075443 (2016).

[11] T. Cheon, A. Tanaka, and S. W. Kim, Phys. Lett. A **374**, 144 (2009).

[12] S. Spurrier and N. R. Cooper, Phys. Rev. A **97**, 043603 (2018).

[13] F. Wilczek and A. Zee, Phys. Rev. Lett. **52**, 2111 (1984).

[14] A. Bohm, A. Mostafazadeh, H. Koizumi, Q. Niu, and Z. Zwanziger, *The Geometric Phase in Quantum Systems* (Springer, Berlin, 2003).

[15] D. Chruściński and A. Jamiołkowski, *Geometric Phases in Classical and Quantum Mechanics* (Birkhäuser, Boston, 2004).

[16] P. Zanardi and M. Rasetti, Phys. Lett. A **264**, 94 (1999).

[17] S. Tanimura, D. Hayashi, and M. Nakahara, Phys. Lett. A **325**, 199 (2004).

[18] E. Sjöqvist, D. M. Tong, L. M. Anderson, B. Hessmo, M. Johansson, and K. Singh, New J. Phys. **14**, 103035 (2012).

[19] E. M. Purcell and R. V. Pound, Phys. Rev. **81**, 279 (1951).

[20] R. Dum, J. I. Cirac, M. Lewenstein, and P. Zoller, Phys. Rev. Lett. **80**, 2972 (1998).

[21] Z. P. Karkuszewski, K. Sacha, and J. Zakrzewski, Phys. Rev. A **63**, 061601(R) (2001).

[22] B. Damski, Z. P. Karkuszewski, K. Sacha, and J. Zakrzewski, Phys. Rev. A **65**, 013604 (2001).

[23] B. Damski, K. Sacha, and J. Zakrzewski, J. Phys. B **35**, L153 (2002).

[24] B. Damski, K. Sacha, and J. Zakrzewski, J. Phys. B **35**, 4051 (2002).

[25] S. Kasumie, M. Miyamoto, and A. Tanaka, Phys. Rev. A **93**, 042105 (2016).

[26] A. Tanaka and T. Cheon, New J. Phys. **18**, 045023 (2016).

[27] T. P. Meyrath, F. Schreck, J. L. Hanssen, C.-S. Chuu, and M. G. Raizen, Phys. Rev. A **71**, 041604(R) (2005).

[28] M. T. Batchelor, X. W. Guan, N. Oelkers, and C. Lee, J. Phys. A. **38**, 7787 (2005).

[29] A. Syrwid and K. Sacha, Phys. Rev. A **96**, 043602 (2017).

[30] M. Sciacca, C. F. Barenghi, and N. G. Parker, Phys. Rev. A **95**, 013628 (2017).

[31] A. Ramanathan, K. C. Wright, S. R. Muniz, M. Zelan, W. T. Hill, III, C. J. Lobb, K. Helmerson, W. D. Phillips, and G. K. Campbell, Phys. Rev. Lett. **106**, 130401 (2011).

[32] F. Piazza, L. A. Collins, and A. Smerzi, Phys. Rev. A **80**, 021601(R) (2009).

[33] M. Kunimi and I. Danshita, Phys. Rev. A **100**, 063617 (2019).

[34] D. J. Frantzeskakis, G. Theocharis, F. K. Diakonos, P. Schmelcher, and Y. S. Kivshar, Phys. Rev. A **66**, 053608 (2002).

[35] I. Hans, J. Stockhofe, and P. Schmelcher, Phys. Rev. A **92**, 013627 (2015).

[36] B. Wu and Q. Niu, Phys. Rev. A **61**, 023402 (2000).

[37] J. Liu, L. Fu, B.-Y. Ou, S.-G. Chen, D.-I. Choi, B. Wu, and Q. Niu, Phys. Rev. A **66**, 023404 (2002).

[38] E. J. Mueller, Phys. Rev. A **66**, 063603 (2002).

[39] M. Kunimi and Y. Kato, Phys. Rev. A **91**, 053608 (2015).

[40] A. Pérez-Obiol and T. Cheon, Phys. Rev. E **101**, 022212 (2020).

[41] T. Kato, J. Phys. Soc. Jpn. **5**, 435 (1950).

[42] B. Simon and T. Wolff, Commun. Pure Appl. Math. **39**, 75 (1986).

[43] J. Gea-Banacloche, Am. J. Phys. **70**, 307 (2001).

[44] N. Bogolubov, J. Phys. (Moscow) **11**, 23 (1947).

[45] A. L. Fetter, Ann. Phys. (NY) **70**, 67 (1972).

[46] B. Wu and Q. Niu, New J. Phys. **5**, 104 (2003).

[47] I. Danshita and S. Tsuchiya, Phys. Rev. A **75**, 033612 (2007).

[48] S. Martínez-Garaot, E. Torrontegui, X. Chen, M. Modugno, D. Guéry-Odelin, S.-Y. Tseng, and J. G. Muga, Phys. Rev. Lett. **111**, 213001 (2013).

[49] S. Masuda, K. Nakamura, and A. del Campo, Phys. Rev. Lett. **113**, 063003 (2014).

[50] S. W. Kim, T. Sagawa, S. De Liberato, and M. Ueda, Phys. Rev. Lett. **106**, 070401 (2011).

[51] V. B. Sørdal and J. Bergli, Phys. Rev. A **99**, 022121 (2019).

[52] W. Kao, K.-Y. Li, K.-Y. Lin, S. Gopalakrishnan, and B. L. Lev, arXiv:2002.10475.